Atmos. Chem. Phys. Discuss., 13, 145–176, 2013
www.atmos-chem-phys-discuss.net/13/145/2013/
doi:10.5194/acpd-13-145-2013

Atmospheric Chemistry and Physics Discussions

Examination of parameterizations for CCN number concentrations based on in-situ aerosol activation property measurements in the North China Plain

Z. Z. Deng[1,2], C. S. Zhao[2], N. Ma[2], L. Ran[1], G. Q. Zhou[3], D. R. Lu[1], and X. J. Zhou[2,4]

[1]Key Laboratory of Middle Atmosphere and Global Environment Observation, Institute of Atmospheric Physics, Chinese Academy of Sciences, Beijing, China
[2]Department of Atmospheric and Oceanic Sciences, School of Physics, Peking University, Beijing, China
[3]Shanghai Typhoon Institute, China Meteorological Administration, Shanghai, China
[4]Centre for Atmosphere Watch and Services, Chinese Academy of Meteorological Sciences, China Meteorological Administration, Beijing, China

Received: 10 November 2012 – Accepted: 19 December 2012 – Published: 4 January 2013

Correspondence to: C. S. Zhao (zcs@pku.edu.cn)

Published by Copernicus Publications on behalf of the European Geosciences Union.

Abstract

Precise quantification of cloud condensation nuclei (CCN) number concentrations is crucial for understanding aerosol indirect effect and characterizing this effect in models. An evaluation of various methods for CCN parameterization is carried out in this paper based on in-situ measurements of aerosol activation properties within HaChi (Haze in China) project. Comparisons are made by closure studies between methods using CCN spectra, bulk activation ratios, cut-off diameters and size-resolved activation ratios. The estimation of CCN number concentrations by the method using aerosol activation curves, either averaged over a day or with diurnal variation, is found to be most satisfying and straightforward. This could be well expected since size-resolved activation ratios include information regarding the effects of size-resolved chemical composition and mixing state on aerosol activation properties. The method using the averages of critical diameters, which are inferred from measured CCN number concentrations and particle number size distribution, also provides a good prediction of CCN number concentrations. Based on comparisons of all these methods in this paper, it is recommended that CCN number concentrations be predicted using particle number size distribution with inferred critical diameters or size-resolved activation ratios.

1 Introduction

Clouds have an impact on the global water cycle by cloud formation and precipitation, also on the energy balance of the earth-atmosphere system by absorption, scattering and emission of radiation. Cloud condensation nuclei (CCN), i.e. the particles that can be activated at a certain water vapor supersaturation, could influence the cloud microphysical properties. The increase of CCN number concentrations may increase cloud droplet number concentrations (Twomey and Warner, 1967; Ramanathan et al., 2001), and decrease the size of cloud droplets (Twomey, 1974), consequently further change cloud lifetime and precipitation (Albrecht, 1989; Zhao et al., 2006b). Thus, CCN number

ACPD
13, 145–176, 2013

concentration is a key factor to characterize the aerosol indirect effects, i.e. the impacts of aerosols as CCN on climate.

CCN number concentrations and CCN spectra have been characterized by field measurements since 1950s (Twomey, 1959a, and reference therein). Measurements in various locations and seasons showed that CCN number concentrations were generally higher in continental air (Delene and Deshler, 2001; Detwiler et al., 2010; Rose et al., 2010; Deng et al., 2011; Gunthe et al., 2011) than in maritime air (Squires and Twomey, 1966; Bigg and Leek, 2001), and higher under polluted conditions than under clean conditions (Hobbs et al., 1980; Snider and Brenguier, 2000; Hudson et al., 2000; Hudson and Yum, 2002). With such high spatial and temporal variability in CCN properties, robust parameterization of CCN number concentrations is of great importance to model applications.

Several parameterization schemes of CCN number concentrations have been developed. Parameterization of CCN spectra with constants (Twomey, 1959b; Ji and Shaw, 1998; Mircea et al., 2005), though simple to carry out, does not take into account any variation in the CCN loading. The bulk activation ratio (the ratio between CCN and aerosol number concentrations) was also a useful parameter in the CCN prediction (Pruppacher and Klett, 1997). Measurements and sensitivity studies indicated that particle size plays a more important role in the aerosol activation process at high supersaturations than chemical composition does (Junge and McLaren, 1971; Fitzgerald, 1973; Dusek et al., 2006), which could however be quite important at low supersaturations (Kuwata et al., 2008; Twohy and Anderson, 2008). Closure studies of CCN number concentrations based on particle number size distributions (PNSD) were conducted to investigate the influence of bulk (Bougiatioti et al., 2009) and size-resolved aerosol chemical compositions (Medina et al., 2007; Stroud et al., 2007). The effects of aerosol mixing states on CCN prediction were also notable in locations with strong anthropogenic aerosol emissions (Ervens et al., 2010; Kammermann et al., 2010; Rose et al., 2010; Wang et al., 2010; Wex et al., 2010; Deng et al., 2011; Kerminen et al.,

ACPD
13, 145–176, 2013

2012). The examination of these methods for CCN calculation can be used to considerably improve the parameterization of CCN number concentrations.

Measurements of aerosol optics (Ma et al., 2011, 2012), aerosol hygroscopicity (Liu et al., 2011) and aerosol activation (Deng et al., 2011) during the Haze in China (HaChi) campaign have shown that the North China Plain (NCP) is one of the most heavily polluted regions in the world, wherein a variety of strong aerosol emission sources are located. Studies show that the high concentrations of aerosol particles in these region may have impacts on cloud microphysical properties and the surface precipitation (Zhao et al., 2006a, b; Deng et al., 2009). Under such polluted circumstances, parameterizations of CCN might be somewhat different from usual methods. Precise quantification of CCN is required in detailed cloud models, where the activation fraction of aerosols depend nonlinearly on the aerosol abundance. Thus, it is necessary to examine the validity of the CCN parameterization schemes. Intensive measurements of aerosol activation properties in this study were employed to evaluate different methods for CCN parameterization, including the use of CCN spectra, bulk CCN activation ratio, cut-off diameters and size-resolved activation ratios (activation curve).

2 Measurements and data

Measurements of PNSD and aerosol activation properties were conducted at Wuqing Meteorological Station from 5 November to 30 December 2011. More information on the site and the polluted surrounding areas were described in Xu et al. (2011) and Ran et al. (2011). Number size distributions and activation properties of aerosols dried to less than 30 % relative humidity were measured by an Aerodynamic Particle Sizer (APS Model 3320, TSI, USA), a Scanning Mobility Particle Sizer (SMPS, Model 3936, TSI, USA) and a continuous-flow CCN counter (CCNC, Model CCN-200, DMT, USA) (Roberts and Nenes, 2005; Lance et al., 2006).

The SMPS consists mainly of a differential mobility analyzer (DMA, Model 3081, TSI, USA) and a condensation particle counter (CPC, Model 3772, TSI, USA). The DMA

ACPD
13, 145–176, 2013

sheath and sample flows were 6 lpm and 0.8 lpm, respectively. The sample flow exiting the DMA was split into two parts, with 0.3 lpm for CPC and 0.5 lpm for one column of the CCNC. The DMA, controlled by the TSI-AIM software, scanned a cycle every five minutes and selected particles in a certain size increment between 10–430 nm. The PNSD and size-resolved activation properties were obtained by using this scanning system (Moore et al., 2010). The PNSD was inverted from the raw counts recorded by AIM using an algorithm (Hagen and Alofs, 1983; Wiedensohler et al., 2012) with the ideal Dirac, triangular transfer function (Knutson and Whitby, 1975) and the particle equilibrium charge probability distribution (Wiedensohler, 1988). The PNSD in the range of 10 nm–10 µm were obtained in combination with APS measurements.

The CCNC column downstream of the DMA was operated at five supersaturations, with 20 min for 0.07 % and 10 min for each of 0.10, 0.20, 0.40 and 0.80 %. The chamber of CCNC was considered as temperature stabilized during the last 5 min of the duration for each supersaturation. The time series of size-selected CCN number concentrations ($N_{CCN,s}(D_p,S)$) during these 5 min were matched with the size-selected CN (Condensation Nuclei) number concentrations ($N_{CN,s}(D_p)$) from CPC. The size-resolved aerosol activation ratios ($A(D_p,S) = N_{CCN,s}(D_p,S)/N_{CN,s}(D_p)$) were inverted from size-selected CCN number concentrations and PNSD using a modified algorithm based on that of Hagen and Alofs (1983). The size-resolved activation ratios for five supersaturations were available every one hour. The sheath and sample flow rates of CCNC were calibrated before the campaign. The supersaturations of CCNC were calibrated with ammonium sulfate (Rose et al., 2008) before and after the campaign. The results showed that the effective supersaturations were 0.061, 0.083, 0.200, 0.414 and 0.812 %, respectively.

The second column of the CCNC was used to measure total CCN number concentrations at supersaturations of 0.07, 0.10, 0.20, 0.40 and 0.80 %, of which direct measurement could lead to considerable underestimation under polluted condition (Deng et al., 2011) due to water depletion inside the column (Lathem and Nenes, 2011). Number size distributions of CCN were constructed by multiplying the PNSD and corresponding

ACPD
13, 145–176, 2013

size-resolved activation ratios. Bulk CCN number concentrations were the integration of CCN number size distributions, and referred to as measured CCN number concentration in the following content.

3 Calculation of CCN number concentrations

The methods for CCN parameterization, including the use of CCN spectra, bulk CCN activation ratio, cut-off diameters and size-resolved activation ratios (activation curve), are compared below to characterize the variations of CCN number concentrations.

3.1 Parameterization of CCN spectra using aerosol number concentration

The method that uses only CCN spectra for CCN parameterization provides a simple way to predict CCN number concentrations, with very few constants required for modeling. CCN supersaturation spectra have often been measured and fitted with different formulas. A commonly used formula,

$$N_{\mathrm{CCN}}(S) = CS^k, \tag{1}$$

was proposed by Twomey (1959b) assuming Junge Power Law Distribution and uniform aerosol chemical composition. This equation contains only two parameters C and k. The parameter C represents CCN number concentrations at supersaturation of 1 %, which are higher in continental and polluted regions than oceanic and clean regions. The parameter k varies more significantly (Martins et al., 2009). Nevertheless, this equation does not fit CCN spectra well. Ji and Shaw (1998) suggested another formula with three parameters N, B and k,

$$N_{\mathrm{CCN}}(S) = N(1 - \exp(-BS^k)), \tag{2}$$

which gave best fitting among several formulas in Mircea et al. (2005).

ACPD
13, 145–176, 2013

Measured CCN spectra in Wuqing were fitted using the two formulas. The probability distribution functions for the fitting parameters are shown in Figs. 1a and 2a. All five fitted parameters varied in a wide range, indicating that it is improper to represent the CCN spectra using constant parameters in models.

The parameters C and N correlated well with aerosol number concentrations (Figs. 1b and 2b), while simple relationships between other parameters and aerosol properties were not found. C and N could thereby be predicted assuming a linear relationship of aerosol number concentrations (diameter larger than 50 nm) $N_{CN,>50\,nm}$, with other parameters set as the averages during the whole campaign. CCN number concentrations were then calculated using the two formulas. Calculated CCN number concentrations correlated well with measurements at high supersaturations, but less correlated at low supersaturations (Figs. 1c and 2c). The slopes of fitted lines between measurements and calculations were far from 1 (0.7–1.7) if the CCN spectra were expressed as formula (1). CCN spectra could not be well represented at low supersaturations even if the parameters vary with aerosol number concentrations. Formula (1) was only capable of predicting CCN number concentrations at supersaturations around 1 %. Formula (2) did not show a systematic estimation bias at either high or low supersaturations. The prediction of CCN number concentrations using either formula correlated poorly with measurements at low supersaturations.

3.2 Calculation of CCN number concentrations using bulk activation ratios

Empirical parameterization of CCN spectra failed mainly because CCN spectra can not be accurately fitted by formulas. Since CCN number concentrations are largely controlled by the population of aerosol particles, we try to improve CCN predictions by relating CCN number concentrations to aerosol number concentrations. A bulk activation ratio (A_{Bulk}) is often used to characterize this relationship, i.e. $A_{Bulk}(S) = N_{CCN,m}(S)/N_{Ref}$, where $N_{CCN,m}(S)$ is the measured CCN number concentration at supersaturation S. The reference aerosol number concentration N_{Ref} usually represents the measured number concentration of particles within measured size range. Since the measured

ACPD
13, 145–176, 2013

aerosol size range might differ in each campaign study, we should keep in mind that the bulk activation ratio derived from N_{Ref} may not be directly comparable. Our bulk activation ratios were obtained using different reference aerosol number concentrations and applied to CCN calculation. Three reference aerosol number concentrations were considered below, namely, (1) total aerosol number concentrations, (2) accumulation mode aerosol number concentrations, and (3) CCN number concentrations assuming ammonium sulfate aerosol.

3.2.1 Using ratios between measured CCN number concentrations and total aerosol number concentrations

Bulk activation ratios derived using total aerosol number concentrations (here we use the number concentration of particles with diameter larger than 10 nm, $N_{CN,>10\,nm}$) ($A_{Bulk,Tot} = N_{CCN,m}(S)/N_{CN,>10\,nm}$) are often reported in literatures. Pruppacher and Klett (1997) summarized previous measurements and indicated that $A_{Bulk,Tot}$ (1 % supersaturation ratio) are in the range of 0.2–0.6 for maritime aerosols and 0.004–0.25 for continental aerosols. Bulk activation ratios measured in the Amazon Basin, however, averaged 0.070, 0.235, 0.458, 0.682 and 0.818 at supersaturations of 0.15, 0.30, 0.60, 1.00 and 1.5 % (Roberts et al., 2002). Bulk activation ratios (based on $N_{CN,3-900\,nm}$) measured near the megacity of Guangzhou in China averaged 0.06, 0.36, 0.53, 0.59, 0.71 and 0.85 at supersaturations of 0.068, 0.27, 0.47, 0.67, 0.87 and 1.27 % (Rose et al., 2010). The average bulk activation ratios (based on $N_{CN,10-460\,nm}$) measured in east Mediterranean were approximately 0.5, 0.7 and 0.8 at supersaturations of 0.21, 0.38 and above 0.5 % (Bougiatioti et al., 2009).

Figure 3a shows the probability distributions (PDF) of bulk activation ratios $A_{Bulk,Tot}$ at different supersaturations in Wuqing. The reference number concentration is the total aerosol number concentration within measured size range of 10 nm–10 µm. Bulk activation ratios at 0.061 and 0.083 % mostly range from nearly 0 to 0.2. Bulk activation ratios at supersaturations above 0.200 % show a large variation, which are probably attributed to the variation of aerosol particle sizes, i.e. the shape of PNSD. Since size-

ACPD
13, 145–176, 2013

resolved activation ratios were relatively stable, bulk activation ratios were larger when the fraction of particles larger than D50 (see Sect. 3.4.1) was larger and vice versa.

Here we examined results of using this ratio to predict CCN number concentrations. Average bulk activation ratios were 0.06, 0.11, 0.37, 0.54 and 0.65 at supersaturations of 0.061, 0.083, 0.200, 0.414 and 0.812 %, respectively. CCN number concentrations were calculated by multiplying total aerosol number concentrations with average bulk activation ratios. The results are shown in Fig. 3b and the slopes of fitted lines and correlation coefficients are listed in Table 1. The correlation coefficients of measured and calculated CCN number concentrations at each supersaturations were mostly below 0.8, with lower values for lower supersaturations. The reference aerosol number concentrations counted in particles that would never be activated at any atmospheric cloud supersaturations, i.e. particles with a diameter of 10–30 nm, within which the number of particles could be either small (accumulation mode dominant condition) or large (new particle formation event). Although these particles are too small to contribute to aerosol activation, they have large impact on the bulk activation ratio. Therefore, it is not a proper method to calculate CCN number concentrations using bulk activation ratios derived from the total aerosol number concentration, especially for low supersaturation conditions.

3.2.2 Using ratios between measured CCN number concentrations and accumulative mode aerosol number concentrations

Bulk activation ratios can also be obtained using measurements of CCN and accumulation mode aerosols. The PNSD of accumulation mode (with diameter larger than 100 nm) aerosols is usually measured by airborne optical particle counters (OPC), such as passive cavity aerosol spectrometer probe (PCASP). Bulk activation ratios derived from PCASP number concentrations range 0.41–0.85 at supersaturations of 0.36 % for the dry season and 0.20–0.45 at supersaturation of 0.28 % for the wet season over southern Africa (Ross et al., 2003). Breed et al. (2002) found bulk activation ratios less than 1 within the boundary layer and larger than 1 above the boundary layer.

ACPD
13, 145–176, 2013

Bulk activation ratios derived from accumulation mode aerosol number concentrations ($N_{CN,Acc}$) ($A_{Bulk,Acc} = N_{CCN,m}(S)/N_{CN,>100\,nm}$) in Wuqing were presented in Fig. 4a. $A_{Bulk,Acc}$ were well below 1 at supersaturations of 0.061 and 0.083 %. $A_{Bulk,Acc}$ at 0.200 % were around 1, because CCN at this supersaturation mainly consist of particles larger than 100 nm. Particles smaller than 100 nm also contribute to CCN at supersaturations of 0.414 and 0.812 %, resulting in $A_{Bulk,Acc}$ above 1.

$A_{Bulk,Acc}$ averaged over the campaign were also used to calculate CCN number concentrations (Fig. 4b). Correlation coefficients of measured and calculated CCN number concentrations were larger than 0.60 at all supersaturations, also larger than those in the case of using $A_{Bulk,Tot}$. Accumulation mode aerosol particles are better indicators of the CCN population than total aerosol particles. The best agreement was achieved at supersaturation of 0.200 %, with the slope of fitted line close to 1 and the correlation coefficient around 0.95. This could be well understood since CCN at supersaturation of 0.200 % were mostly composed of particles larger than 100 nm. At other supersaturations, correlations between measured and calculated CCN number concentrations were not as good as that at supersaturation of 0.200 %. This is because particles irrelevant for aerosol activation were included at lower supersaturations and particles prone to be activated at higher supersaturations were omitted when accumulation mode particles were used as reference particles.

3.2.3 Using ammonium sulfate as reference aerosol composition

The applications of $A_{Bulk,Tot}$ and $A_{Bulk,Acc}$ showed that it is of great importance to choose appropriate size ranges of the reference number concentrations for bulk activation ratios in CCN number concentration calculation. A fixed size range might be suitable for one supersaturation but inadequate for the others. Therefore, choosing different size ranges of reference number concentrations for different supersaturations might improve the application of bulk activation ratios in CCN number concentration calculation.

The hygroscopic growth and activation behavior of ammonium sulfate can be predicted theoretically (Low 1969; Young and Warren, 1992; Tang and Munkelwitz, 1994),

ACPD
13, 145–176, 2013

and often used in instrument calibration. Here, we propose a method using ammonium sulfate as a reference substance to represent the overall aerosol activation properties. CCN number concentration ($N_{CCN,AS}(S)$) at supersaturation S was calculated by integrating the PNSD with diameters greater than the ammonium sulfate critical diameter at S, assuming that all particles were composed of 100 % ammonium sulfate and taken as reference number concentration. The bulk activation ratio derived from these reference CCN number concentrations ($A_{Bulk,AS} = N_{CCN,m}(S)/N_{CCN,AS}(S)$) roughly represents the fraction of ammonium sulfate in an external mixture with insoluble material.

The probability distribution of $A_{Bulk,AS}$ is displayed in Fig. 5a. $A_{Bulk,AS}$ is above 0.7 at supersaturations of 0.200 % and higher, whereas it was only about 0.4 at lower supersaturations as a result of less soluble materials contained in larger particles. CCN number concentrations were even better predicted by the method using average $A_{Bulk,AS}$ during the campaign than the two methods introduced in Sects. 3.2.1 and 3.2.2 (Fig. 5b). The slopes of fitted line were close to 1. The correlation coefficients between calculated and measured CCN number concentrations were 0.83 and 0.86 at supersaturations of 0.061 % and 0.083 %, and above 0.90 at supersaturations of 0.200 % and higher.

3.3 Calculation of CCN number concentrations using inferred critical diameter

The methods presented in above sections used measurements of CCN and aerosol number concentrations for CCN parameterization. Besides aerosol number concentrations, the size of aerosols was another important factor for controlling CCN number concentrations. In this section, the PNSD of aerosols were included to improve the calculation of CCN number concentrations.

With an assumption of uniform, internally mixed but unspecified chemical composition throughout the size range, a critical dry particle diameter (D_{inf}) can be inferred from measured CCN number concentration and PNSD, namely, the integral of PNSD larger than D_{inf} equals to the measured CCN number concentration. Particles with diameter larger than D_{inf} can be activated at a given supersaturation, while smaller ones can not.

ACPD
13, 145–176, 2013

Results were shown in Fig. 6a. At two lower supersaturations, the probability distribution functions of the inferred critical diameters were comparable to those in Deng et al. (2011). At higher supersaturations, PDFs had two peaks in Deng et al. (2011), while only one peak in this study. A wider range of D_{inf} in last paper corresponded to water depletion in CCNC (Lathem and Nenes, 2011). Bulk CCN number concentrations were underestimated when abundant aerosol particles were activated, which would result in overestimated inferred critical diameter.

Average inferred critical diameter for each supersaturation was used as a cut-off diameter to calculate CCN number concentrations (Fig. 6b). Surprisingly, calculated CCN number concentrations matched well with measured ones. The slopes of fitted lines were 0.96, 0.98, 1.00, 1.01 and 1.01 for supersaturations of 0.061, 0.083, 0.200, 0.414 and 0.812 %, respectively. The correlation coefficients were above 0.8 at all supersaturations. These results suggest that the method using inferred critical diameters is capable of easily and precisely predicting CCN number concentrations.

3.4 Calculation of CCN number concentrations using size-resolved activation ratios

Size-resolved activation ratios, combined with PNSD, provide a straightforward way to calculate CCN number concentrations. Size-resolved activation ratios depend on aerosol chemical composition and aerosol mixing state, which are not usually available through measurements or models. Here several methods for CCN parameterization are examined using measured size-resolved activation ratios.

3.4.1 Using D50 derived from activation curves

Size-resolved activation ratios provide another cut-off diameter for CCN calculation. A critical diameter, denoted as D_{50}, is often derived from measured size-resolved activation ratios. D_{50} is the diameter below which 50 % of the aerosol particles are activated. Multiply-charged particles can influence the determination of D_{50}. If the mode

ACPD
13, 145–176, 2013

diameter of the polydisperse size distribution exceeds the critical diameter of the particles, multiply-charged particles may lead to nonmonotonic CCN counter response curves (Petters et al., 2007). Frank et al. (2006) and Deng et al. (2011) have proposed procedures for multiple charge correction. Size-resolved activation ratios in this study were inverted to eliminate the effects of multiply charge and DMA transfer function.

D_{50} of a simple sigmoidally-shaped activation curve is determined by fitting the size-resolved activation ratios with a formula as below,

$$A(D_p) = d / \left\{1 + \exp\left[(D_{50} - D_p)/a\right]\right\}, \quad (3)$$

where $A(D_p)$ is the activation ratio of particles with diameter D_p, a and d are fitting constants. The maximum activation ratios d are not always 1, due to the measurement uncertainty and sometimes insufficient size range. Thus, D_{50} is usually defined as the diameter below which $0.5d$ of the aerosol particles are activated.

Figure 7a presents the PDF of D_{50}. The average D_{50}, namely 214.5, 175.1, 93.1, 60.9 and 45.4 nm at each supersaturation, were lower than the inferred critical dry diameter (Fig. 7b). There are three possible reasons for such difference.

First, the activation curves were not sigmoidally shaped. The activation curve measured in the North China Plain, in both this study (Fig. 8a) and Deng et al. (2011), were not ideal sigmoidally shaped. Measured activation ratios were lower than that which a sigmoidal function would give at the diameters where activation ratios were close to the maximum. Similar activation curves have also been found in Beijing (Gunther et al. 2011). Such non-sigmoidally shaped activation curves resulted from the externally mixed aerosols. Assuming a flat PNSD ($\mathrm{d}N/\mathrm{d}\log D_p$ is constant), lower activation ratios at diameters above D_{50} due to less hygroscopic particles would lead to $D_{inf} > D_{50}$.

Second, the PNSD were not flat. If D_{50} was smaller than the peak diameter (in the case of higher supersaturations), $D_{inf} > D_{50}$, while $D_{inf} < D_{50}$ if D_{50} was larger than the peak diameter (in the case of lower supersaturations).

Third, D_{inf} might be larger than D_{50}, when the maximum activation ratios were lower than 1 for the reason of measurement uncertainty and insufficient measuring range.

ACPD
13, 145–176, 2013

Application of D_{50} (either real-time or campaign average) to calculating CCN number concentrations resulted in an overestimation of about 20 % (Fig. 7c, d). Based on these results, prediction of CCN number concentration might be biased due to the improper determination of D_{50} for externally mixed aerosol.

3.4.2 Using averaged activation curves without diurnal variation

Similar to the inferred critical diameter, D_{50} is derived assuming a uniform aerosol chemical composition. However, aerosols in the North China Plain were found to be usually externally mixed (Liu et al., 2011). Size-resolved activation ratios, which contain information on aerosol mixing state, are hopefully to improve the CCN calculation.

Average size-resolved activation ratios during the campaign are shown in Fig. 8a. To test how well the average condition represents size-resolved activation properties of aerosols, the temporal variations of the activation curves are not considered. CCN number concentrations calculated using measured PNSD and average size-resolved activation ratios are shown in Fig. 8b. Measured and calculated CCN number concentrations were linearly fitted. The slopes of fitted lines and correlation coefficients at different supersaturations are given in Table 1. The calculation slightly underestimates CCN number concentrations, and correlation coefficients are bellow 0.9 at supersaturations of 0.061 and 0.083 %, at which size-resolved activation ratios display a larger variability than that at higher supersaturations. The slopes of fitted lines are close to 1 and the correlation coefficients are above 0.95 at supersaturations of 0.200 % and higher. The method using average size-resolved activation ratios to calculate CCN number concentrations generally provides a reasonable estimation.

3.4.3 Using averaged activation curves with diurnal variation

Size-resolved activation ratios had strong diurnal variations at lower supersaturations (Fig. 9a). Emissions in rush hours increased the amount of particles with low hygroscopicity and resulted in lower activation ratios. The increase of activation ratios in

ACPD
13, 145–176, 2013

daytime was due to aerosol aging. The maximum activation ratios within the measured size range varied significantly at low supersaturations, e.g. 0.6–0.9 and 0.75–1.0 at supersaturations of 0.061 and 0.083 %. However, D50 did not show such large variability.

Figure 9b displays CCN number concentrations calculated taking account of the diurnal variation of size-resolved activation ratios. The slopes of the fitted lines were similar to those calculated without considering the diurnal variation of size-resolved activation ratios, whereas the correlation coefficients were a little higher.

4 Summary and conclusion

In this paper, methods for calculating CCN number concentrations based on aerosol size distributions (summarized in Table 1) were examined using a dataset from HaChi field campaign in the North China Plain.

The method using CCN spectra to predict CCN number concentrations was easy to be used in models. However, the parameters in fitted functions for CCN spectra span over a wide range. Reasonable results of CCN spectra could only be obtained using the number concentration of aerosols with diameter larger than 50 nm at high supersaturations. There is inevitable limitation of using this method for CCN prediction under very clean and polluted conditions, since aerosol size distribution and chemical composition are not properly accounted for in this method.

The method using bulk activation ratios together with aerosol number concentrations provide a simple way to calculate CCN number concentrations. Results showed that the ratio between measured CCN number concentration and total/accumulation mode aerosol number concentration significantly varied. With the assumption that the aerosol is an external mixture of ammonium sulfate and CCN-inactive substances, we proposed a new parameterization of CCN number concentrations.

The cut-off diameter divided particles into the CCN-active group and the CCN-inactive group. D50 was often obtained from size resolved activation ratios and applied in the calculation of CCN number concentrations. Calculated CCN number concen-

ACPD
13, 145–176, 2013

trations were generally overestimated by about 15–20 % because of non-sigmoidally shaped activation curves and the non-flat PNSD. Inferred critical dry diameters were inversely calculated, assuming a homogeneous chemical composition. CCN number concentrations can be well predicted by using campaign-averaged inferred critical dry diameters at each supersaturation.

For above methods, aerosol chemical composition and mixing state was assumed. However, ambient aerosols had size-dependent compositions and were often partially externally mixed. The aerosol activation curves included information on aerosol chemical compositions and mixing states, and could thereby be used to reasonably predict CCN number concentrations on the basis of PNSD. Results showed that the campaign-averaged activation curves could well predict CCN number concentrations. Moreover, the agreement between calculated and measured CCN number concentrations was even better when the diurnal variation of size-resolve activation ratios was taken into account.

Based on the criteria that correlation coefficients of calculated and measured CCN number concentrations are above 0.8 and the fitted slopes between 0.9–1.1, it is recommended to predict CCN number concentrations using PNSD together with inferred critical diameter or size-resolved activation ratios.

Acknowledgement. This work is supported by the National 973 Project of China (2011CB403402), and the National Natural Science Foundation of China (NSFC) under grants 41205098 and 41005007. This work is also supported by the Meteorology Foundation GYHY200906025, GYHY201006011 and the “Strategic Priority Research Program” of the Chinese Academy of Sciences (XDA05100000).

ACPD
13, 145–176, 2013

References

Albrecht, B. A.: Aerosols, cloud microphysics, and fractional cloudiness, Science, 245, 1227–1230, doi:10.1126/science.245.4923.1227, 1989.

Bigg, E. K. and Leek, C.: Cloud-active particles over the central Arctic Ocean, J. Geophys. Res., 106, 32155–32166, doi:10.1029/1999jd901152, 2001.

Bougiatioti, A., Fountoukis, C., Kalivitis, N., Pandis, S. N., Nenes, A., and Mihalopoulos, N.: Cloud condensation nuclei measurements in the marine boundary layer of the Eastern Mediterranean: CCN closure and droplet growth kinetics, Atmos. Chem. Phys., 9, 7053–7066, doi:10.5194/acp-9-7053-2009, 2009.

Breed, D., Bruintjes, R., Jensen, T., Salazar, V., and Piketh, S.: Aerosol and cloud droplet measurements in the United Arab Emirates, 11th Conference on Cloud Physics, 2002.

Delene, D. J. and Deshler, T.: Vertical profiles of cloud condensation nuclei above Wyoming, J. Geophys. Res., 106, 12579–12588, doi:10.1029/2000jd900800, 2001.

Deng, Z. Z., Zhao, C. S., Ma, N., Liu, P. F., Ran, L., Xu, W. Y., Chen, J., Liang, Z., Liang, S., Huang, M. Y., Ma, X. C., Zhang, Q., Quan, J. N., Yan, P., Henning, S., Mildenberger, K., Sommerhage, E., Schäfer, M., Stratmann, F., and Wiedensohler, A.: Size-resolved and bulk activation properties of aerosols in the North China Plain, Atmos. Chem. Phys., 11, 3835–3846, doi:10.5194/acp-11-3835-2011, 2011.

Deng, Z., Zhao, C., Zhang, Q., Huang, M., and Ma, X.: Statistical analysis of microphysical properties and the parameterization of effective radius of warm clouds in Beijing area, Atmos. Res., 93, 888–896, 2009.

Detwiler, A., Langerud, D., and Depue, T.: Investigation of the variability of cloud condensation nuclei concentrations at the surface in Western North Dakota, J. Appl. Meteorol. Clim., 49, 136–145, 2010.

Dusek, U., Frank, G. P., Hildebrandt, L., Curtius, J., Schneider, J., Walter, S., Chand, D., Drewnick, F., Hings, S., Jung, D., Borrmann, S., and Andreae, M. O.: Size matters more than chemistry for cloud-nucleating ability of aerosol particles, Science, 312, 1375–1378, doi:10.1126/science.1125261, 2006.

Ervens, B., Cubison, M. J., Andrews, E., Feingold, G., Ogren, J. A., Jimenez, J. L., Quinn, P. K., Bates, T. S., Wang, J., Zhang, Q., Coe, H., Flynn, M., and Allan, J. D.: CCN predictions using simplified assumptions of organic aerosol composition and mixing state: a synthesis from

ACPD
13, 145–176, 2013

six different locations, Atmos. Chem. Phys., 10, 4795–4807, doi:10.5194/acp-10-4795-2010, 2010.
Fitzgerald, J. W.: Dependence of the supersaturation spectrum of CCN on aerosol size distribution and composition, J. Atmos. Sci., 30, 628–634, 1973.
Frank, G. P., Dusek, U., and Andreae, M. O.: Technical note: A method for measuring size-resolved CCN in the atmosphere, Atmos. Chem. Phys. Discuss., 6, 4879–4895, doi:10.5194/acpd-6-4879-2006, 2006.
Gunthe, S. S., Rose, D., Su, H., Garland, R. M., Achtert, P., Nowak, A., Wiedensohler, A., Kuwata, M., Takegawa, N., Kondo, Y., Hu, M., Shao, M., Zhu, T., Andreae, M. O., and Pöschl, U.: Cloud condensation nuclei (CCN) from fresh and aged air pollution in the megacity region of Beijing, Atmos. Chem. Phys., 11, 11023–11039, doi:10.5194/acp-11-11023-2011, 2011.
Hagen, D. E. and Alofs, D. J.: Linear inversion method to obtain aerosol size distributions from measurements with a differential mobility analyzer, Aerosol Sci. Tech., 2, 465–475, 1983.
Hobbs, P. V., Stith, J. L., and Radke, L. F.: Cloud-active nuclei from coal-fired electric power plants and their interactions with clouds, J. Appl. Meteorol., 19, 439–451, doi:10.1175/1520-0450(1980)019<0439:canfcf>2.0.co;2, 1980.
Hudson, J. G. and Yum, S. S.: Cloud condensation nuclei spectra and polluted and clean clouds over the Indian Ocean, J. Geophys. Res., 107, 8022, doi:10.1029/2001jd000829, 2002.
Hudson, J. G., Garrett, T. J., Hobbs, P. V., Strader, S. R., Xie, Y., and Yum, S. S.: Cloud condensation nuclei and ship tracks, J. Atmos. Sci., 57, 2696–2706, doi:10.1175/1520-0469(2000)057<2696:CCNAST>2.0.CO;2, 2000.
Ji, Q. and Shaw, G. E.: On supersaturation spectrum and size distributions of cloud condensation nuclei, Geophys. Res. Lett., 25, 1903–1906, doi:10.1029/98gl01404, 1998.
Junge, C. and McLaren, E.: Relationship of cloud nuclei spectra to aerosol size distribution and composition, J. Atmos. Sci., 28, 382–390, 1971.
Kammermann, L., Gysel, M., Weingartner, E., Herich, H., Cziczo, D. J., Holst, T., Svenningsson, B., Arneth, A., and Baltensperger, U.: Subarctic atmospheric aerosol composition: 3. Measured and modeled properties of cloud condensation nuclei, J. Geophys. Res., 115, D04202, doi:10.1029/2009jd012447, 2010.
Kerminen, V.-M., Paramonov, M., Anttila, T., Riipinen, I., Fountoukis, C., Korhonen, H., Asmi, E., Laakso, L., Lihavainen, H., Swietlicki, E., Svenningsson, B., Asmi, A., Pandis, S. N., Kulmala, M., and Petäjä, T.: Cloud condensation nuclei production associated with atmospheric

ACPD
13, 145–176, 2013

nucleation: a synthesis based on existing literature and new results, Atmos. Chem. Phys., 12, 12037–12059, doi:10.5194/acp-12-12037-2012, 2012.
Knutson, E. O. and Whitby, K. T.: Aerosol classification by electric mobility: apparatus, theory, and applications, J. Aerosol Sci., 6, 443–451, 1975.
Kuwata, M., Kondo, Y., Miyazaki, Y., Komazaki, Y., Kim, J. H., Yum, S. S., Tanimoto, H., and Matsueda, H.: Cloud condensation nuclei activity at Jeju Island, Korea in spring 2005, Atmos. Chem. Phys., 8, 2933–2948, doi:10.5194/acp-8-2933-2008, 2008.
Lance, S., Medina, J., Smith, J. N., and Nenes, A.: Mapping the operation of the DMT continuous flow CCN counter, Aerosol Sci. Tech., 40, 242–254, 2006.
Lathem, T. L. and Nenes, A.: Water vapor depletion in the DMT continuous-flow CCN chamber: effects on supersaturation and droplet growth, Aerosol Sci. Tech., 45, 604–615, doi:10.1080/02786826.2010.551146, 2011.
Liu, P. F., Zhao, C. S., Göbel, T., Hallbauer, E., Nowak, A., Ran, L., Xu, W. Y., Deng, Z. Z., Ma, N., Mildenberger, K., Henning, S., Stratmann, F., and Wiedensohler, A.: Hygroscopic properties of aerosol particles at high relative humidity and their diurnal variations in the North China Plain, Atmos. Chem. Phys., 11, 3479–3494, doi:10.5194/acp-11-3479-2011, 2011.
Low, R. D. H.: A generalized equation for the solution effect in droplet growth, J. Atmos. Sci., 26, 608–611, 1969.
Ma, N., Zhao, C. S., Nowak, A., Müller, T., Pfeifer, S., Cheng, Y. F., Deng, Z. Z., Liu, P. F., Xu, W. Y., Ran, L., Yan, P., Göbel, T., Hallbauer, E., Mildenberger, K., Henning, S., Yu, J., Chen, L. L., Zhou, X. J., Stratmann, F., and Wiedensohler, A.: Aerosol optical properties in the North China Plain during HaChi campaign: an in-situ optical closure study, Atmos. Chem. Phys., 11, 5959–5973, doi:10.5194/acp-11-5959-2011, 2011.
Ma, N., Zhao, C. S., Müller, T., Cheng, Y. F., Liu, P. F., Deng, Z. Z., Xu, W. Y., Ran, L., Nekat, B., van Pinxteren, D., Gnauk, T., Müller, K., Herrmann, H., Yan, P., Zhou, X. J., and Wiedensohler, A.: A new method to determine the mixing state of light absorbing carbonaceous using the measured aerosol optical properties and number size distributions, Atmos. Chem. Phys., 12, 2381–2397, doi:10.5194/acp-12-2381-2012, 2012.
Martins, J., Gonçalves, F., Morales, C., Fisch, G., Pinheiro, F., Leal Júnior, J., Oliveira, C., Silva, E., Oliveira, J., Costa, A., and Silva Dias, M.: Cloud condensation nuclei from biomass burning during the Amazonian dry-to-wet transition season, Meteorol. Atmos. Phys., 104, 83–93, 2009.

ACPD
13, 145–176, 2013

Medina, J., Nenes, A., Sotiropoulou, R.-E. P., Cottrell, L. D., Ziemba, L. D., Beckman, P. J., and Griffin, R. J.: Cloud condensation nuclei closure during the International Consortium for Atmospheric Research on Transport and Transformation 2004 campaign: effects of size-resolved composition, J. Geophys. Res., 112, D10S31, doi:10.1029/2006jd007588, 2007.

Mircea, M., Facchini, M. C., Decesari, S., Cavalli, F., Emblico, L., Fuzzi, S., Vestin, A., Rissler, J., Swietlicki, E., Frank, G., Andreae, M. O., Maenhaut, W., Rudich, Y., and Artaxo, P.: Importance of the organic aerosol fraction for modeling aerosol hygroscopic growth and activation: a case study in the Amazon Basin, Atmos. Chem. Phys., 5, 3111–3126, doi:10.5194/acp-5-3111-2005, 2005.

Moore, R. H., Nenes, A., and Medina, J.: Scanning mobility CCN analysis – a method for fast measurements of size-resolved CCN distributions and activation kinetics, Aerosol Sci. Tech., 44, 861–871, 2010.

Petters, M. D., Prenni, A. J., Kreidenweis, S. M., and DeMott, P. J.: On measuring the critical diameter of cloud condensation nuclei using mobility selected aerosol, Aerosol Sci. Tech., 41, 907–913, 2007.

Pruppacher, H. R. and Klett, J. D.: Microphysics of Clouds and Precipitation, Kluwer Academic Publishers, Dordrecht, The Netherlands, 944 pp., 1997.

Ramanathan, V., Crutzen, P. J., Kiehl, J. T., and Rosenfeld, D.: Aerosols, climate, and the hydrological cycle, Science, 294, 2119–2124, doi:10.1126/science.1064034, 2001.

Ran, L., Zhao, C. S., Xu, W. Y., Lu, X. Q., Han, M., Lin, W. L., Yan, P., Xu, X. B., Deng, Z. Z., Ma, N., Liu, P. F., Yu, J., Liang, W. D., and Chen, L. L.: VOC reactivity and its effect on ozone production during the HaChi summer campaign, Atmos. Chem. Phys., 11, 4657–4667, doi:10.5194/acp-11-4657-2011, 2011.

Roberts, G. C. and Nenes, A.: A continuous-flow streamwise thermal-gradient CCN chamber for atmospheric measurements, Aerosol Sci. Tech., 39, 206–221, 2005.

Roberts, G. C., Artaxo, P., Zhou, J., Swietlicki, E., and Andreae, M. O.: Sensitivity of CCN spectra on chemical and physical properties of aerosol: a case study from the Amazon Basin, J. Geophys. Res., 107, 8070, doi:10.1029/2001jd000583, 2002.

Rose, D., Gunthe, S. S., Mikhailov, E., Frank, G. P., Dusek, U., Andreae, M. O., and Pöschl, U.: Calibration and measurement uncertainties of a continuous-flow cloud condensation nuclei counter (DMT-CCNC): CCN activation of ammonium sulfate and sodium chloride aerosol particles in theory and experiment, Atmos. Chem. Phys., 8, 1153–1179, doi:10.5194/acp-8-1153-2008, 2008.

ACPD
13, 145–176, 2013

Rose, D., Nowak, A., Achtert, P., Wiedensohler, A., Hu, M., Shao, M., Zhang, Y., Andreae, M. O., and Pöschl, U.: Cloud condensation nuclei in polluted air and biomass burning smoke near the mega-city Guangzhou, China – Part 1: Size-resolved measurements and implications for the modeling of aerosol particle hygroscopicity and CCN activity, Atmos. Chem. Phys., 10, 3365–3383, doi:10.5194/acp-10-3365-2010, 2010.

Ross, K. E., Piketh, S. J., Bruintjes, R. T., Burger, R. P., Swap, R. J., and Annegarn, H. J.: Spatial and seasonal variations in CCN distribution and the aerosol-CCN relationship over southern Africa, J. Geophys. Res., 108, 8481, doi:10.1029/2002jd002384, 2003.

Snider, J. R. and Brenguier, J. L.: Cloud condensation nuclei and cloud droplet measurements during ACE-2, Tellus B, 52, 828–842, 2000.

Squires, P. and Twomey, S.: A comparison of cloud nucleus measurements over Central North America and the Caribbean Sea, J. Atmos. Sci., 23, 401–404, doi:10.1175/1520-0469(1966)023<0401:acocnm>2.0.co;2, 1966.

Stroud, C. A., Nenes, A., Jimenez, J. L., DeCarlo, P. F., Huffman, J. A., Bruintjes, R., Nemitz, E., Delia, A. E., Toohey, D. W., Guenther, A. B., and Nandi, S.: Cloud activating properties of aerosol observed during CELTIC, J. Atmos. Sci., 64, 441–459, 2007.

Tang, I. N. and Munkelwitz, H. R.: Water activities, densities, and refractive indices of aqueous sulfates and sodium nitrate droplets of atmospheric importance, J. Geophys. Res., 99, 801–808, 1994.

Twohy, C. H. and Anderson, J. R.: Droplet nuclei in non-precipitating clouds: composition and size matter, Environ. Res. Lett., 3, 045002, doi:10.1088/1748-9326/3/4/045002, 2008.

Twomey, S.: The nuclei of natural cloud formation part I: The chemical diffusion method and its application to atmospheric nuclei, Pure Appl. Geophys., 43, 227–242, 1959a.

Twomey, S.: The nuclei of natural cloud formation part II: The supersaturation in natural clouds and the variation of cloud droplet concentration, Pure Appl. Geophys., 43, 243–249, 1959b.

Twomey, S.: Pollution and the planetary albedo, Atmos. Environ., 8, 1251–1256, 1974.

Twomey, S. and Warner, J.: Comparison of Measurements of Cloud Droplets and Cloud Nuclei, J. Atmos. Sci., 24, 702–703, doi:10.1175/1520-0469(1967)024<0702:COMOCD>2.0.CO;2, 1967.

Wang, J., Cubison, M. J., Aiken, A. C., Jimenez, J. L., and Collins, D. R.: The importance of aerosol mixing state and size-resolved composition on CCN concentration and the variation of the importance with atmospheric aging of aerosols, Atmos. Chem. Phys., 10, 7267–7283, doi:10.5194/acp-10-7267-2010, 2010.

ACPD
13, 145–176, 2013

Wex, H., McFiggans, G., Henning, S., and Stratmann, F.: Influence of the external mixing state of atmospheric aerosol on derived CCN number concentrations, Geophys. Res. Lett., 37, 10805, doi:10.1029/2010GL043337, 2010.

Wiedensohler, A.: An approximation of the bipolar charge distribution for particles in the submicron size range, J. Aerosol Sci., 19, 387–389, 1988.

Wiedensohler, A., Birmili, W., Nowak, A., Sonntag, A., Weinhold, K., Merkel, M., Wehner, B., Tuch, T., Pfeifer, S., Fiebig, M., Fjäraa, A. M., Asmi, E., Sellegri, K., Depuy, R., Venzac, H., Villani, P., Laj, P., Aalto, P., Ogren, J. A., Swietlicki, E., Williams, P., Roldin, P., Quincey, P., Hüglin, C., Fierz-Schmidhauser, R., Gysel, M., Weingartner, E., Riccobono, F., Santos, S., Grüning, C., Faloon, K., Beddows, D., Harrison, R., Monahan, C., Jennings, S. G., O'Dowd, C. D., Marinoni, A., Horn, H. G., Keck, L., Jiang, J., Scheckman, J., McMurry, P. H., Deng, Z., Zhao, C. S., Moerman, M., Henzing, B., de Leeuw, G., Löschau, G., and Bastian, S.: Mobility particle size spectrometers: harmonization of technical standards and data structure to facilitate high quality long-term observations of atmospheric particle number size distributions, Atmos. Meas. Tech., 5, 657–685, doi:10.5194/amt-5-657-2012, 2012.

Xu, W. Y., Zhao, C. S., Ran, L., Deng, Z. Z., Liu, P. F., Ma, N., Lin, W. L., Xu, X. B., Yan, P., He, X., Yu, J., Liang, W. D., and Chen, L. L.: Characteristics of pollutants and their correlation to meteorological conditions at a suburban site in the North China Plain, Atmos. Chem. Phys., 11, 4353–4369, doi:10.5194/acp-11-4353-2011, 2011.

Young, K. C. and Warren, A. J.: A reexamination of the derivation of the equilibrium supersaturation curve for soluble particles, J. Atmos. Sci., 49, 1138–1143, 1992.

Zhao, C., Tie, X., Brasseur, G., Noone, K. J., Nakajima, T., Zhang, Q., Zhang, R., Huang, M., Duan, Y., Li, G., and Ishizaka, Y.: Aircraft measurements of cloud droplet spectral dispersion and implications for indirect aerosol radiative forcing, Geophys. Res. Lett., 33, L16809, doi:10.1029/2006gl026653, 2006a.

Zhao, C., Tie, X., and Lin, Y.: A possible positive feedback of reduction of precipitation and increase in aerosols over eastern central China, Geophys. Res. Lett., 33, L11814, doi:10.1029/2006gl025959, 2006b.

ACPD
13, 145–176, 2013

Table 1. Comparison of different methods.

Category	Principle	Details	R^2	Slope
CCN spectra	The parameters in the formula are expressed as a function of N_{CN} ($D > 50$ nm)	$N_{CCN} = CS^k$	0.90 (0.46–0.98)	0.92 (0.70–1.87)
		$N_{CCN} = N_0(1 - \exp(-BS^k))$	0.96 (0.43–0.98)	1.02 (0.86–1.18)
Bulk activation ratio $A_{Bulk} = N_{CCN}/N_{Ref}$	$N_{CN} * A_{Bulk,Mean}$	$N_{Ref} = N_{CN,>10nm}$	0.88 (0.25–0.83)	0.91 (0.81–0.95)
		$N_{Ref} = N_{CN,>100nm}$	0.94 (0.67–0.96)	1.08 (0.86–1.16)
		$N_{Ref} = N_{CCN,AS}(S)$	**0.98 (0.83–0.96)**	**0.96 (0.91–0.97)**
Cut-off diameter	Use a cut-off diameter to distinguish CCN-active and CCN-inactive particles	Critical dry diameter D_{inf} is inferred from the measured PNSD and $N_{CCN,m}$. Campaign average D_{inf} is used	**0.99 (0.86–0.98)**	**1.01 (0.96–1.01)**
		D_{50}, real-time	0.99 (0.92–0.99)	1.18 (1.16–1.32)
		D_{50}, campaign average	0.99 (0.86–0.98)	1.17 (1.16–1.30)
Size-resolved activation ratios	$n_{CN}(D_p) * A(D_p)$ $\rightarrow n_{CCN}(D_p)$ $\rightarrow N_{CCN}$	Campaign average of the activation curves	**0.99 (0.86–0.98)**	**1.00 (0.94–1.00)**
		Diurnal variation of the activation curves	**0.99 (0.88–0.98)**	**0.99 (0.95–1.00)**

ACPD
13, 145–176, 2013

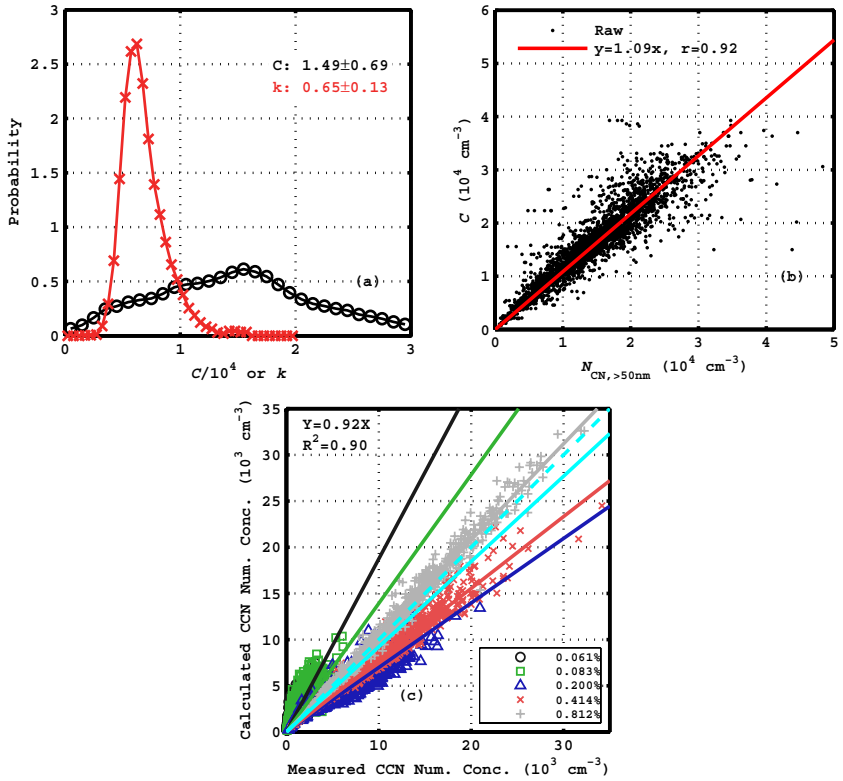

Fig. 1. Fitted results of $N_{CCN} = CS^k$ and their application to calculation of CCN number concentrations. **(a)** PDF of fitting parameters. The numbers are average values and corresponding standard deviation. **(b)** Linear relationship between aerosol (larger than 50 nm) number concentration and fitting parameter C. **(c)** Prediction of CCN number concentration. The scattered data are the pairs of measurement and calculation, with one color for each supersaturation. The linearly fitted lines are shown with corresponding colors. The cyan beeline is linear fitted line for all the data. The cyan dashed line is 1 : 1 line.

ACPD
13, 145–176, 2013

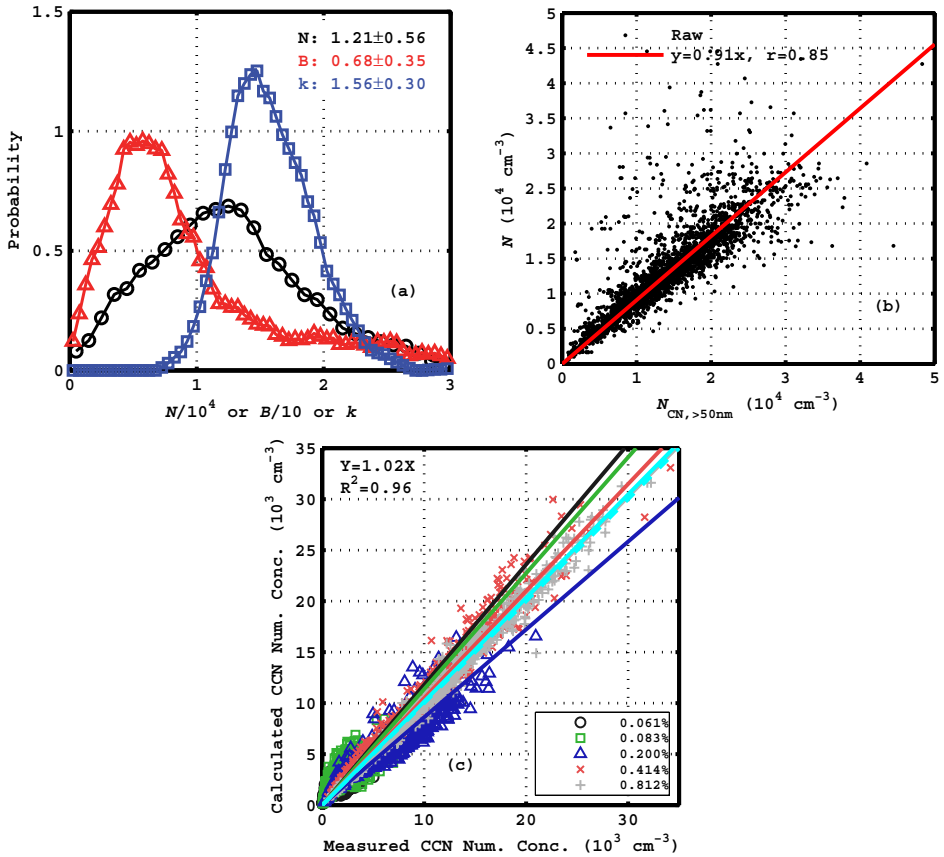

Fig. 2. Fitted results of $N_{CCN} = N(1 - \exp(-BS^k))$ and their application to calculation of CCN number concentrations. **(a)** PDF of fitting parameters; **(b)** linear relationship between aerosol (larger than 50 nm) number concentration and fitting parameter N; **(c)** prediction of CCN number concentration.

ACPD
13, 145–176, 2013

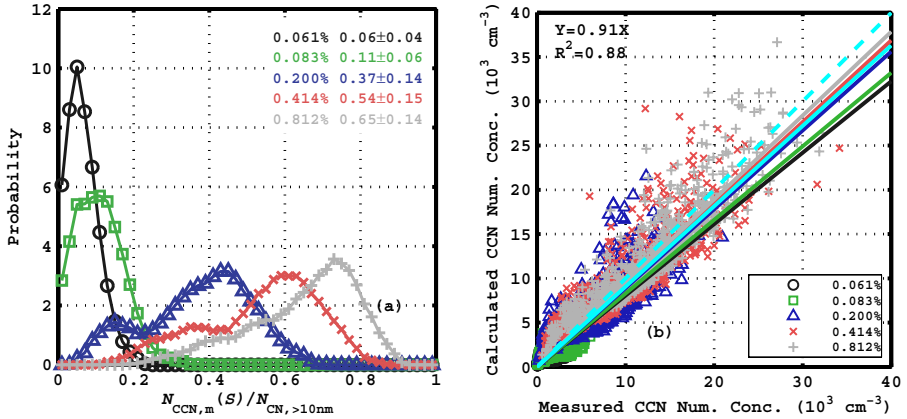

Fig. 3. (a) PDF of total number based bulk activation ratio $N_{CCN,m}(S)N_{CN,>10nm}$ and **(b)** their application of mean $N_{CCN,m}(S)N_{CN,>10nm}$ to calculation of CCN number concentrations.

ACPD
13, 145–176, 2013

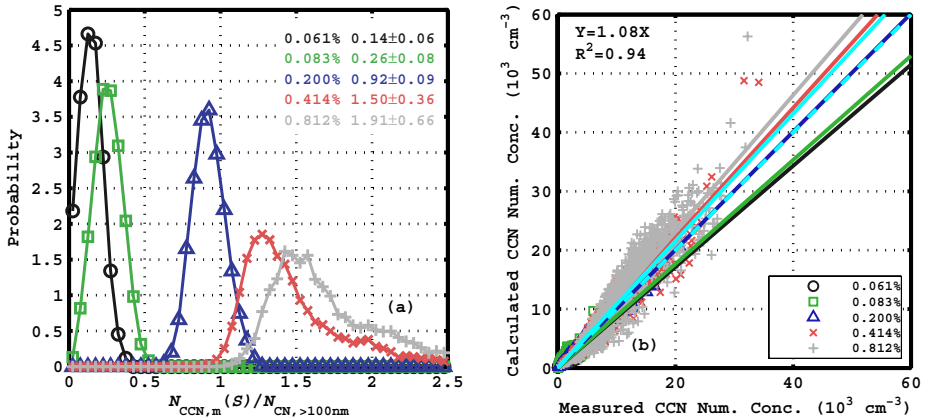

Fig. 4. (a) PDF of accumulation mode number based bulk activation ratio $N_{CCN,m}(S)/N_{CN,>100nm}$ and **(b)** their application of mean $N_{CCN,m}(S)/N_{CN,>100nm}$ to calculation of CCN number concentrations.

ACPD
13, 145–176, 2013

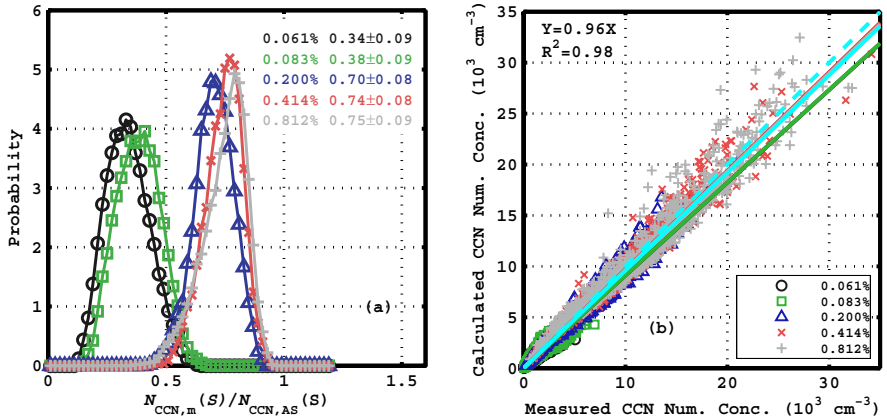

Fig. 5. (a) PDF of $N_{CCN,m}(S)/N_{CCN,AS}(S)$ and **(b)** their application of mean $N_{CCN,m}(S)/N_{CCN,AS}(S)$ to calculation of CCN number concentrations.

ACPD
13, 145–176, 2013

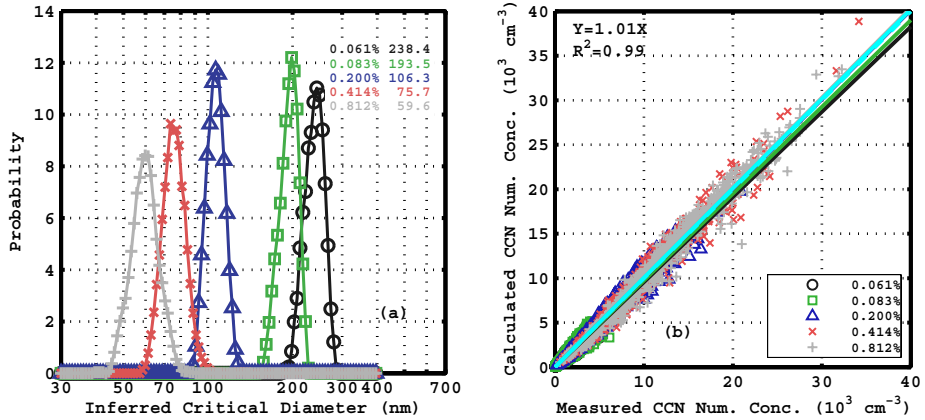

Fig. 6. (a) PDF of inferred critical diameters and **(b)** their application to calculation of CCN number concentrations.

ACPD
13, 145–176, 2013

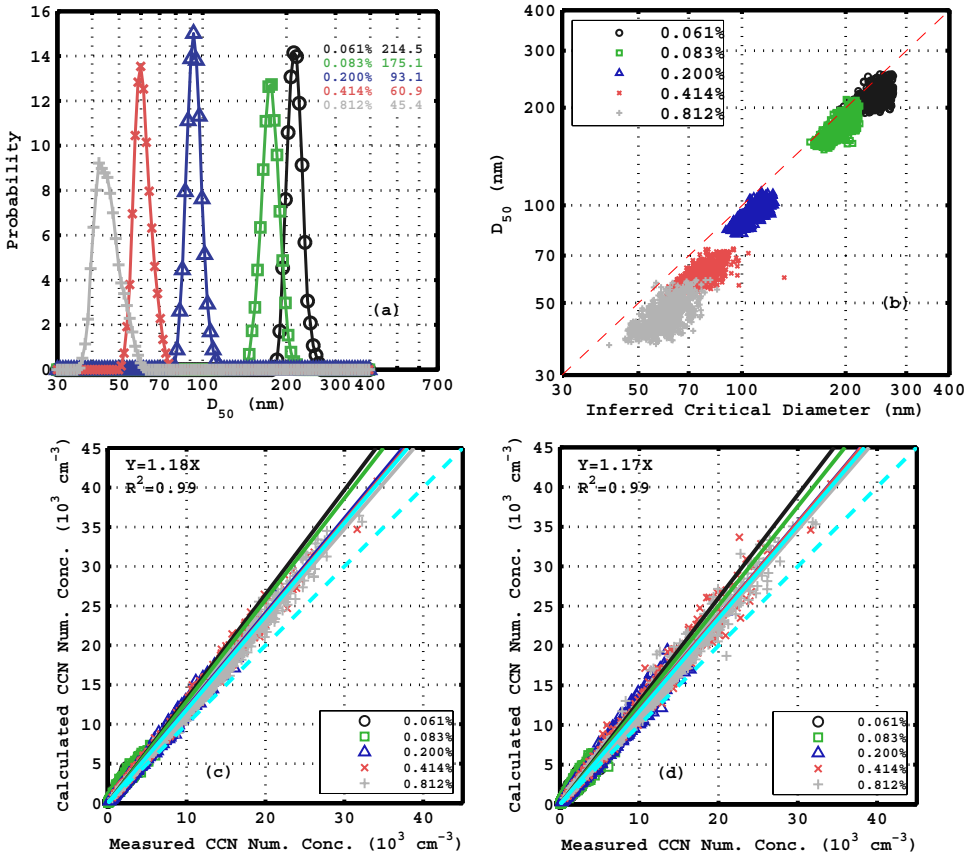

Fig. 7. D_{50} and their application to calculation of CCN number concentrations. **(a)** PDF of D_{50}; **(b)** relationship between D_{50} and D_{inf}; **(c)** the application of real-time D_{50}; **(d)** the application of cammpaign-average D_{50}.

ACPD
13, 145–176, 2013

Examination of parameterizations for CCN number concentrations

Z. Z. Deng et al.

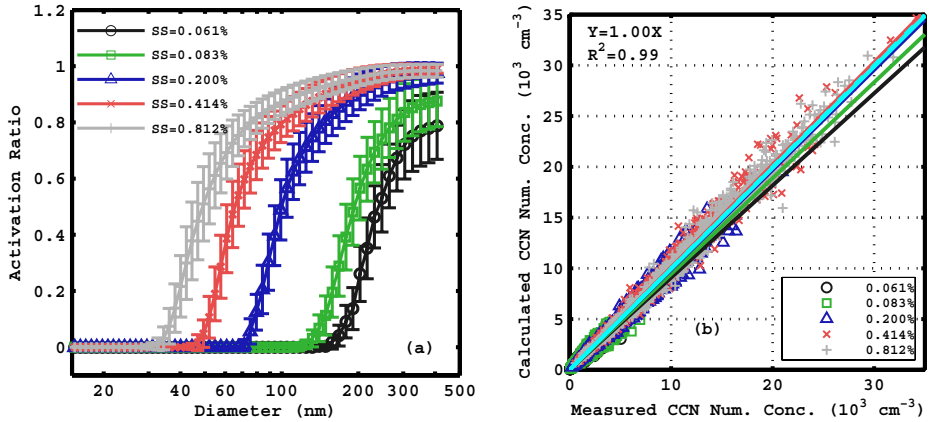

Fig. 8. (a) Average size-resolved activation ratios and **(b)** their application to calculation of CCN number concentrations.

ACPD
13, 145–176, 2013

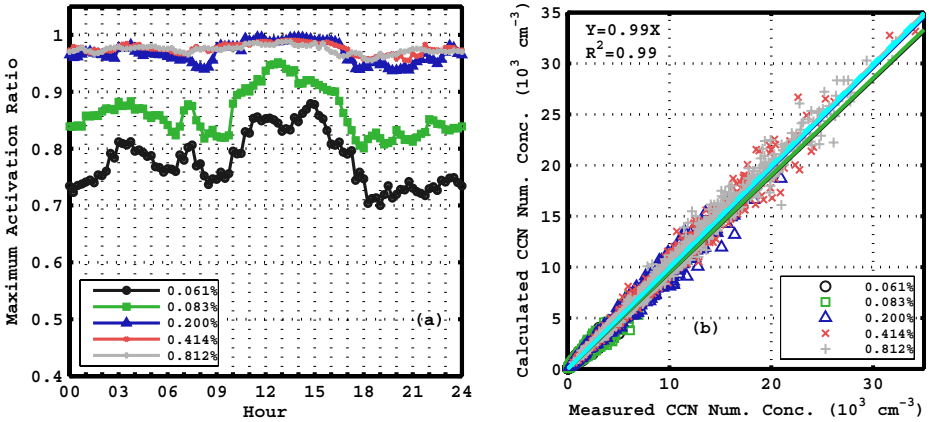

Fig. 9. (a) Diurnal variation of maximum of size-resolved activation ratios and **(b)** their application to calculation of CCN number concentrations.

ACPD
13, 145–176, 2013